

By making the rotating wave approximation¹⁰, we find equations with analytic solutions for the resonant case. The conductivity induced by a rectangular pulse of duration τ is taken to be proportional to $(1 - \rho_{11}(\tau))$, the total number of donors excited out of the ground state at the end of the terahertz pulse. The solid curves in Fig. 3a are a least-squares fit of the data to this analytic solution. The fitted curves reproduce the essential features of the data.

The inset to Fig. 3a shows the Rabi frequency and damping rates extracted from the fits as functions of E_{THz} . If we assume a dipole matrix element of 10 nm, then the Rabi frequency at a terahertz field of $3.1 \times 10^4 \text{ V m}^{-1}$ is predicted to be $4.7 \times 10^{11} \text{ rad s}^{-1}$, well within experimental error of the observed value. The fitted Rabi frequency increases roughly linearly with E_{THz} but with a non-zero intercept. The magnetic field was tuned to be resonant at the highest E_{THz} . The non-zero intercept is consistent with the detuning that results from the shift in the resonance frequency with E_{THz} (see Fig. 3b).

We calculated the curves in Fig. 4b by fixing the model parameters with a fit to the on-resonance curve, and varying only the detuning for the off-resonance curves. The frequency of the oscillations in the theoretical curves increases with increasing detuning, while the amplitude decreases, as observed in the experiment; however, we note that the amplitude decreases much more quickly with detuning in the experiment.

The mechanisms that damp the observed Rabi oscillations are extrinsic to the model qubits, and much faster than predicted intrinsic decoherence. The value of the dephasing rate γ_2 at the lowest terahertz field is, within experimental error, the same as that obtained from the linear spectra, $60 \times 10^9 \text{ s}^{-1}$. This regime is inhomogeneously broadened by a background disorder potential¹⁶. As the terahertz field is increased, the inset to Fig. 3a shows γ_2 and γ_3 increasing, consistent with a photoionization process that couples the $2p^+$ state to a higher excited state. Intrinsic decoherence of motional states of hydrogenic impurities is expected to be limited by very weak coupling to acoustic phonons^{3,22–24}. From table III of ref. 23, the contribution of acoustic-phonon coupling to the line-width (full-width at half-maximum, FWHM) of the $1s-2p$ ($m=0$) transition at zero magnetic field is predicted to be $\leq 10^{-3} \Xi^2 / (\rho a^3 v^2) \approx 0.2 \mu\text{eV}$ (where $\Xi = 8.6 \text{ eV}$ is the deformation potential, $a = 10 \text{ nm}$ is the Bohr radius, $\rho = 5,300 \text{ kg m}^{-3}$ is the density, and $v = 3,700 \text{ m s}^{-1}$ is the velocity of sound, corresponding to an intrinsic decoherence rate $\gamma_2 \leq 2 \times 10^8 \text{ s}^{-1}$. Such decoherence rates, more than 1,000 times slower than typical Rabi frequencies measured here, would enable more complex manipulations of the model qubits. Future experiments will attempt to measure the intrinsic decoherence time of $2p$ ($m=-1$) hydrogenic donor states, which are well below the continuum and hence robust to ionization by photons and phonons. □

Received 5 December; accepted 18 December 2000.

- Loss, D. & DiVincenzo, D. P. Quantum computation with quantum dots. *Phys. Rev. A* **57**, 120–126 (1998).
- Kane, B. E. A silicon-based nuclear spin quantum computer. *Nature* **393**, 133–137 (1998).
- Sherwin, M. S., Imamoglu, A. & Montroy, T. Quantum computation with quantum dots and terahertz cavity quantum electrodynamics. *Phys. Rev. A* **60**, 3508–3514 (1999).
- Imamoglu, A. *et al.* Quantum information processing using quantum dot spins and cavity QED. *Phys. Rev. Lett.* **83**, 4204–4207 (1999).
- Vrijen, R. *et al.* Electron spin resonance transistors for quantum computing in silicon-germanium hetero-structures. Preprint quant-ph/9905096 at (<http://xxx.lanl.gov>) (1999).
- Bennett, C. H. & DiVincenzo, D. P. Quantum information and computation. *Nature* **404**, 247–255 (2000).
- DiVincenzo, D. P. Quantum computation. *Science* **270**, 255–261 (1995).
- Hegmann, F. A. *et al.* Time-resolved photoresponse of a gallium-doped germanium photoconductor using a variable pulse-width terahertz source. *Appl. Phys. Lett.* **76**, 262–264 (2000).
- Rabi, I. I. Space quantization in a gyrating magnetic field. *Phys. Rev.* **51**, 652–654 (1937).
- Boyd, R. W. *Nonlinear Optics* (Academic, Boston, 1992).
- Kohn, W. in *Solid State Physics* (eds Seitz, F. & Turnbull, D.) Vol. 5, 257–320 (Academic, New York, 1957).
- Yu, P. Y. & Cardona, M. *Fundamentals of Semiconductors: Physics and Materials Properties* (Springer, Berlin, 1999).
- Klaassen, T. O., Dunn, J. L. & Bates, C. A. in *Atoms and Molecules in Strong External Fields* (eds

- Schmelcher, P. & Schweizer, W.) 291–300 (Plenum, New York, 1998).
- Stillman, G. E., Wolfe, C. M. & Dimmock, J. O. Magnetospectroscopy of shallow donors in GaAs. *Solid State Commun.* **7**, 921–925 (1969).
- Burghoorn, J., Klaassen, T. O. & Wenckebach, W. T. The dynamics of shallow donor ionization in n-GaAs studied with sub-ps FIR-induced photoconductivity. *Semicond. Sci. Technol.* **9**, 30–34 (1994).
- Larsen, D. M. Inhomogeneous line broadening in donor magneto-optical spectra. *Phys. Rev. B* **8**, 535–553 (1973).
- Planken, P. C. M. *et al.* Far-infrared picosecond time-resolved measurement of the free-induction decay in GaAs:Si. *Phys. Rev. B* **51**, 9643–9647 (1995).
- Cundiff, S. T. *et al.* Rabi flopping in semiconductors. *Phys. Rev. Lett.* **73**, 1178–1181 (1994).
- Schulzgen, A. *et al.* Direct observation of excitonic Rabi oscillations in semiconductors. *Phys. Rev. Lett.* **82**, 2346–2349 (1999).
- Ramian, G. The new UCSB free-electron lasers. *Nucl. Instrum. Methods Phys. Res. A* **318**, 225–229 (1992).
- Hegmann, F. A. & Sherwin, M. S. Generation of picosecond far-infrared pulses using laser activated semiconductor reflection switches. *Proc. SPIE* **2842**, 90–105 (1996).
- Bockelmann, U. Phonon scattering between zero-dimensional electronic states: Spatial versus Landau quantization. *Phys. Rev. B* **50**, 17271–17279 (1994).
- Barrie, R. & Nishikawa, K. Phonon broadening of impurity spectral lines II. Application to silicon. *Can. J. Phys.* **41**, 1823–1835 (1963).
- Nishikawa, K. & Barrie, R. Phonon broadening of impurity spectral lines I. General theory. *Can. J. Phys.* **41**, 1135–1173 (1963).
- Stanley, C. R. *et al.* Electrical characterization of molecular beam epitaxial GaAs with peak electron mobilities up to approximately $4 \times 10^5 \text{ cm}^2 \text{ V}^{-1} \text{ s}^{-1}$. *Appl. Phys. Lett.* **58**, 478–480 (1991).
- Stanley, C. R., Holland, M. C., Hutchins, R. H., Kean, A. H. & Johnson, N. P. in *Institute of Physics Conference Series* Vol. 112 (ed. Singer, K. E.) 67–72 (IOP Publishing, London, 1990).
- McKnight, S. W., Stewart, K. P., Drew, H. D. & Moorjani, K. Wavelength-independent anti-interference coating for the far-infrared. *Infrared Phys.* **27**, 327–333 (1987).

Acknowledgements

We thank D. K. Enyeart and C. Sean Roy for assistance with experiments, and C. J. Weinberger, D. D. Awschalom, and A. Imamoglu for critical readings of the manuscript. This work was supported by the ARO, the ONR/Medical Free-Electron Laser Program, the NSF, and Sun Microsystems.

Correspondence and requests for materials should be addressed to M.S.S. (e-mail: sherwin@physics.ucsb.edu).

Superconductivity at 39 K in magnesium diboride

Jun Nagamatsu*, Norimasa Nakagawa*, Takahiro Muranaka*, Yuji Zenitani* & Jun Akimitsu*†

* Department of Physics, Aoyama-Gakuin University, Chitosedai, Setagaya-ku, Tokyo 157-8572, Japan

† CREST, Japan Science and Technology Corporation, Kawaguchi, Saitama 332-0012, Japan

In the light of the tremendous progress that has been made in raising the transition temperature of the copper oxide superconductors (for a review, see ref. 1), it is natural to wonder how high the transition temperature, T_c , can be pushed in other classes of materials. At present, the highest reported values of T_c for non-copper-oxide bulk superconductivity are 33 K in electron-doped $\text{Cs}_x\text{Rb}_{1-x}\text{C}_{60}$ (ref. 2), and 30 K in $\text{Ba}_{1-x}\text{K}_x\text{BiO}_3$ (ref. 3). (Hole-doped C_{60} was recently found⁴ to be superconducting with a T_c as high as 52 K, although the nature of the experiment meant that the supercurrents were confined to the surface of the C_{60} crystal, rather than probing the bulk.) Here we report the discovery of bulk superconductivity in magnesium diboride, MgB_2 . Magnetization and resistivity measurements establish a transition temperature of 39 K, which we believe to be the highest yet determined for a non-copper-oxide bulk superconductor.

The samples were prepared from powdered magnesium (Mg; 99.9%) and powdered amorphous boron (B; 99%) in a dry box. The powders were mixed in an appropriate ratio (Mg:B = 1:2), ground and pressed into pellets. The pellets were heated at 973 K

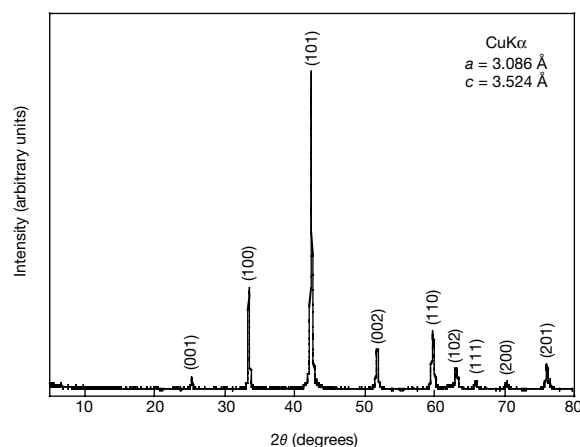


Figure 1 X-ray diffraction pattern of MgB_2 at room temperature.

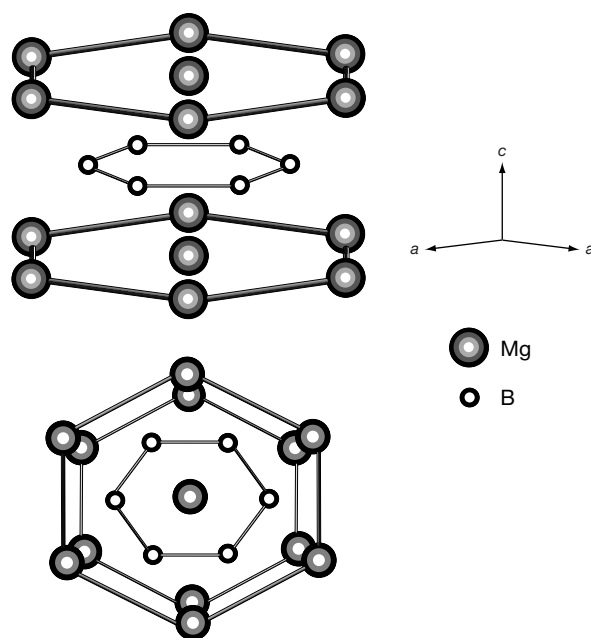


Figure 2 Crystal structure of MgB_2 .

under a high argon pressure, 196 MPa, using a hot isostatic pressing (HIP) furnace ($\text{O}_2\text{Dr.HIP}$, Kobelco) for 10 hours. Powder X-ray diffraction was performed by a conventional X-ray spectrometer with a graphite monochromator (RINT-2000, Rigaku). Intensity data were collected with $\text{CuK}\alpha$ radiation over a 2θ range from 5° to 80° at a step width of 0.02° .

Figure 1 shows a typical X-ray diffraction pattern of MgB_2 taken at room temperature. All the intense peaks can be indexed assuming an hexagonal unit cell, with $a = 3.086 \text{ \AA}$ and $c = 3.524 \text{ \AA}$. Figure 2 shows the crystal structure of MgB_2 (ref. 5), of which the space group is $P6/mmm$ (no.191). As shown in Fig. 2, the boron atoms are arranged in layers, with layers of Mg interleaved between them. The structure of each boron layer is the same as that of a layer in the graphite structure: each boron atom is here equidistant from three other boron atoms. Therefore, MgB_2 is composed of two layers of boron and magnesium along the c axis in the hexagonal lattice.

Magnetization measurements were also performed with a SQUID magnetometer (MPMSR2, Quantum Design). Figure 3 shows the magnetic susceptibility ($\chi = M/H$, where M is magnetization and H is magnetic field) of MgB_2 as a function of temperature, under

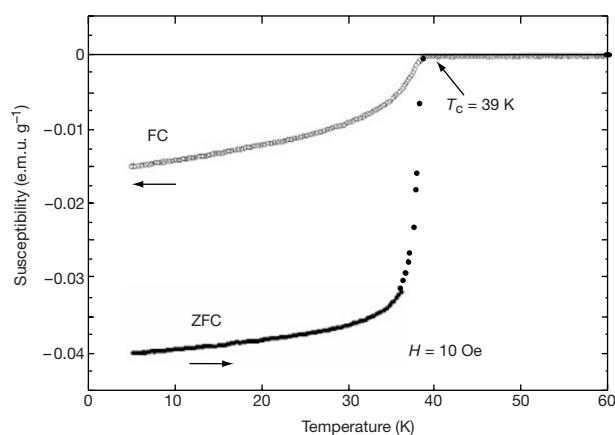


Figure 3 Magnetic susceptibility χ of MgB_2 as a function of temperature. Data are shown for measurements under conditions of zero field cooling (ZFC) and field cooling (FC) at 10 Oe.

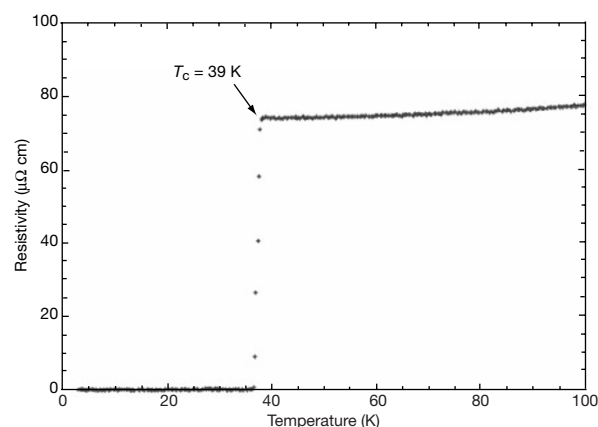


Figure 4 Temperature dependence of the resistivity of MgB_2 under zero magnetic field.

conditions of zero field cooling (ZFC) and field cooling (FC) at 10 Oe. The existence of the superconducting phase was then confirmed unambiguously by measuring the Meissner effect on cooling in a magnetic field. The onset of a well-defined Meissner effect was observed at 39 K. A superconducting volume fraction of 49% under a magnetic field of 10 Oe was obtained at 5 K, indicating that the superconductivity is bulk in nature. The standard four-probe technique was used for resistivity measurements.

Figure 4 shows the temperature dependence of the resistivity of MgB_2 under zero magnetic field. The onset and end-point transition temperatures are 39 K and 38 K, respectively, indicating that the superconductivity was truly realized in this system. □

Received 24 January; accepted 5 February 2001.

1. Takagi, H. in *Proc. Int. Conf. on Materials and Mechanisms of Superconductivity, High Temperature Superconductors VI*. Physica C **341-348**, 3–7 (2000).
2. Tanigaki, K. *et al.* Superconductivity at 33 K in $\text{Cs}_x\text{Rb}_{1-x}\text{C}_{60}$. *Nature* **352**, 222–223 (1991).
3. Cava, R. V. *et al.* Superconductivity near 30 K without copper: the $\text{Ba}_{0.6}\text{K}_{0.4}\text{BiO}_3$ perovskite. *Nature* **332**, 814–816 (1988).
4. Schön, J. H., Kloc, Ch. & Batlogg, B. Superconductivity at 52 K in hole-doped C_{60} . *Nature* **408**, 549–552 (2000).
5. Jones, M. & Marsh, R. The preparation and structure of magnesium boride, MgB_2 . *J. Am. Chem. Soc.* **76**, 1434–1436 (1954).

Acknowledgements

This work was partially supported by a Grant-in-Aid for Science Research from the Ministry of Education, Science, Sports and Culture, Japan and by a grant from CREST.

Correspondence and requests for materials should be addressed to J.A. (e-mail: jun@soliton.phys.aoyama.ac.jp).